ASTRONOMY & ASTROPHYSICS
SUPPLEMENT SERIES

Astron. Astrophys. Suppl. Ser. **128,** 131-138 (1998)

Photometric study of the open cluster NGC 2323⋆,⋆⋆

J.J. Clariá, A.E. Piatti, and E. Lapasset

Observatorio Astronómico, Universidad Nacional de Córdoba, Laprida 854, 5000 Córdoba, Argentina

Received April 2; accepted June 18, 1997

Abstract. UBV photoelectric photometry for 175 stars in the field of the southern open cluster NGC 2323, supplemented by DDO photometry of 5 probable giants, is presented. The analysis of the photometric data yields 109 probable members; one of them being a red giant, and 3 possible members. The reddening across the cluster is slightly variable and the mean value $E(B-V) = 0.25$. The apparent cluster distance modulus is 10.62, corresponding to a distance of 940 pc. The age, determined by fitting isochrones with core overshooting, turns out to be 100 ± 20 Myr. Other fundamental cluster parameters are also determined. NGC 2323 appears not to be physically connected to the CMa OB1 association.

Key words: open clusters: individual: NGC 2323 — open clusters: general — HR diagram

1. Introduction

The study of open clusters located in the direction of stellar associations and/or extended gas regions is of great interest in different astrophysical aspects. By analysing clusters physically connected with them it is possible to investigate the internal and environmental conditions during the star formation processes (see, e.g., Caillault 1994; Shaoguang 1995; Henning et al. 1995). The information that could be obtained about the structure, spatial mass distribution, and initial luminosity function of these clusters, constitutes an important tool to the knowledge of what happened since their births until the present (Massey et al. 1995; Murray & Lin 1996). On the other hand, if the clusters are not connected with stellar associations - which are generally related to HII regions - one can argue about the uneffectiveness of the star formation in those zones of the galactic disk.

As part of a program dealing with the spatial distribution of O and B stars in Canis Major, Clariá (1972, 1973) studied photometrically two open clusters (NGC 2335 and NGC 2343) located in the direction of the CMa OB1 association. He suggested that both clusters most likely form a double system. Their estimated distances (1050 pc and 960 pc, respectively) and the one of 1150 pc derived by Clariá (1974b) for CMa OB1 suggest a possible physical relation between the clusters and CMa OB1. However, the ages derived for the clusters ($\approx$ 100 Myr) make it highly improbable that these clusters and the association could have been originated from the same protostellar material.

NGC 2323 (OCI-559, $l = 221.7^{\circ}$, $b = -1.3^{\circ}$), located nearly at the edge of CMa OB1, could be another candidate belonging to the association. This cluster was studied by several authors using photographic photometry (see, e.g., Cuffey 1941; Hoag et al. 1961; Mostafa et al. 1983), who placed it between 520 pc (Rieke 1935) and 1170 pc (Hoag et al. 1961) from the sun. Although the age of NGC 2323 was determined by Barbaro et al. (1969) and Mostafa et al. (1983), there is no agreement between both estimations. In fact, the former derived an age of (6 ± 1) 10^7 yr, whereas the latter obtained 1.4 10^8 yr.

In order to perform a better determination of the cluster parameters as well as to clarify the probable connection of NGC 2323 to CMa OB1, we have carried out UBV photoelectric photometry in the cluster field. Five probable red giants were also observed in the DDO system to evaluate cluster membership and to derive reddening and metal content. In Sect. 2 we describe the observations and the data reduction. The analysis of the UBV and DDO photometric data is presented in Sects. 3 and 4. In Sects. 5 and 6 we derive age and discuss the cluster luminosity function. Finally, in Sect. 7 we analyze the possible connection of NGC 2323 to CMa OB1. The principal results of the present study are summarized in Table 6.

Send offprint requests to: J.J. Clariá,
e-mail: claria@oac.uncor.edu

⋆ Based on observations made at Cerro Tololo Inter-American Observatory (Chile) and at Las Campanas Observatory (Chile).

⋆⋆ Tables 1 and 2 are only available in electronic form at the CDS via anonymous ftp to cdsarc.u-strasbg.fr (130.79.128.5) or via http://cdsweb.u-strasbg.fr/Abstract.html

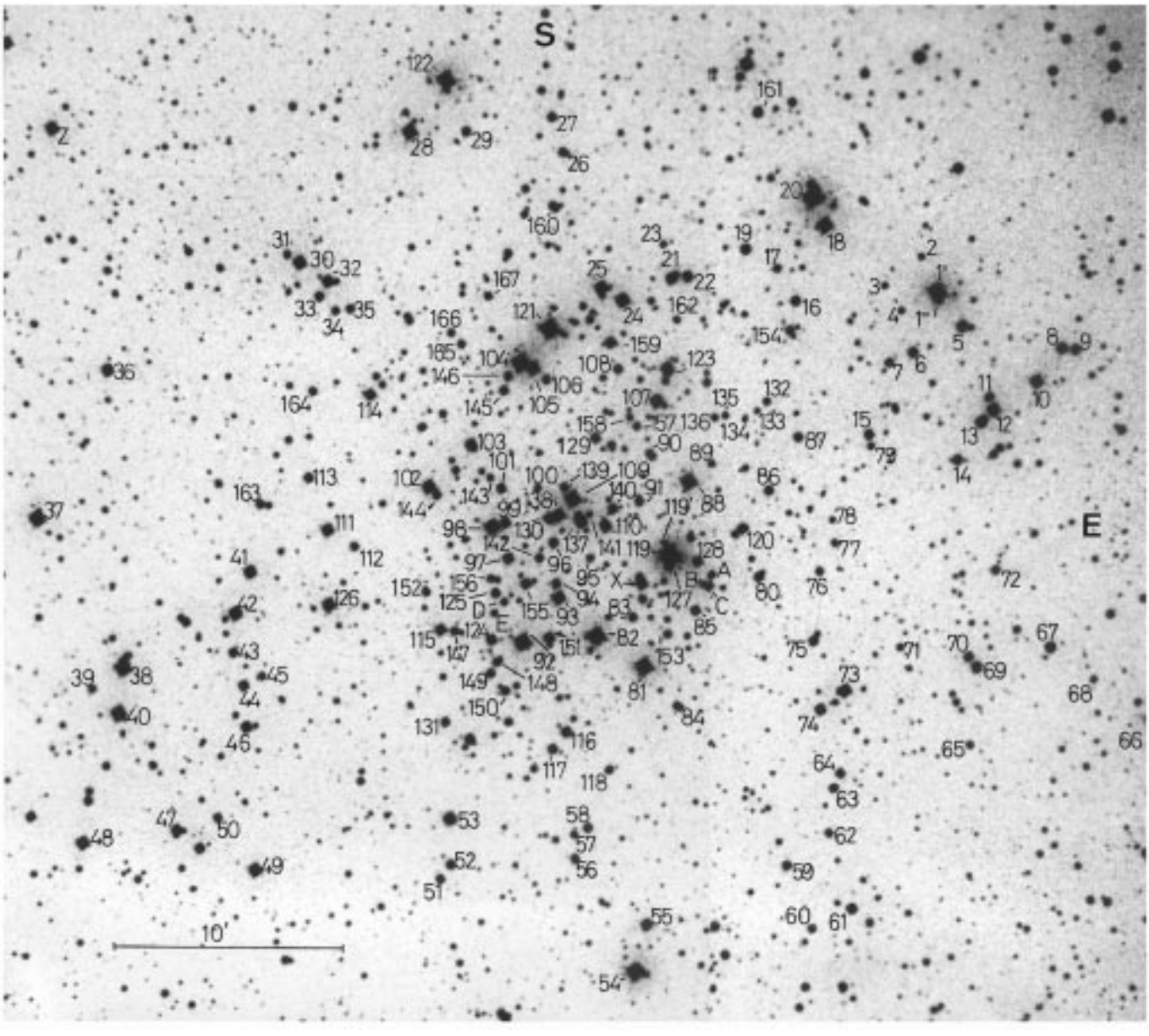

Fig. 1. Identification chart for stars in NGC 2323

2. Observations and reductions

UBV photoelectric observations of a total of 175 stars in the field of NGC 2323 were collected with the University of Toronto's 0.6 m telescope at Las Campanas Observatory (LCO) and with the Cerro Tololo Inter-American Observatory (CTIO) 0.9-m telescope, over a large number of photometric nights from March 1984 to February 1987. Dry-ice cooled RCA 1P21 and Ga-As RCA 31034 phototubes in single channel photometers with pulse-counting electronics were used for all observations at LCO and CTIO, respectively. Mean extinction coefficients at both observatories were employed and nightly observations of about 13-17 standard stars taken from the lists of Cousins (1973, 1974), Landolt (1973) and Graham (1982) were used to transform instrumental magnitudes into the UBV standard system. External and internal mean errors are nearly similar to those in previous papers (e.g., Clariá et al. 1991). Typically $\sigma V \leq 0.014$ mag, $\sigma B-V \leq 0.010$ mag and $\sigma U-B \leq 0.017$ mag for $V < 12$ mag, increasing to 0.018, 0.022 and 0.027 for $V > 12$ mag, respectively. Table 1 lists V magnitudes, $U-B$ and $B-V$ colours, and the number of measurements performed in each filter for all the stars numbered in Fig. 1, while Table 2 includes the correlation of identifications with other authors.

We compare our photoelectric photometry with the most extensive and recent photographic survey carried out by Mostafa et al. (1983). As can be seen in Fig. 2, there

is no colour dependence between the magnitude scales, an appreciable scatter being the principal feature. The resulting mean differences (in the sense Mostafa et al. minus this study) for a total of 66 stars in common are -0.005 ± 0.239, -0.029 ± 0.138 and 0.025 ± 0.112 for the U, B and V magnitudes, respectively.

In addition, observations of five stars in the DDO system were carried out with the purpose of obtaining additional information about their reddening, probable membership, luminosity class, and metal content. These measurements were made in April 1985 using the CTIO 0.9-m telescope with an S − 20 photomultiplier. The transformation to the DDO standard system was done by nightly observing between 12 to 16 standards from the list of McClure (1976). All the measurements were performed with a single-channel photometer and pulse counting electronics. The resulting external mean errors in the DDO colours were found to be about or slightly smaller than 0.01 mag. In Table 3 we list the DDO colours obtained for each star and the number n of individual observations.

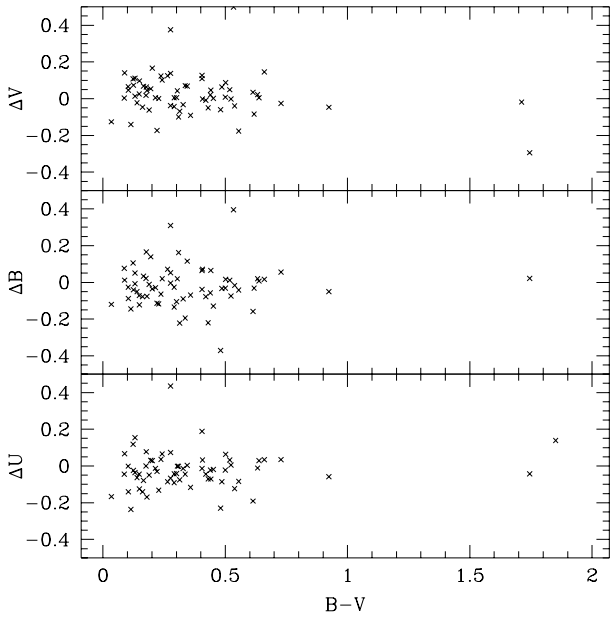

Fig. 2. Magnitude differences (Mostafa et al. minus this study) versus photoelectric colours

3. *UBV* analysis

3.1. Membership criteria

Figures 3 and 4 show the two colour-magnitude (CM) diagrams for all the measured stars, wherein the solid line represents the zero age main sequence (ZAMS) taken from Schmidt-Kaler (1982). Both CM diagrams reveal the presence of a reasonably broad and slightly evolved main sequence (MS), typical of an early intermediate-age open cluster. The MS extends over a range of nearly 6 magnitudes, with the faintest stars at $V \approx 14.5$ mag. The CM diagrams also show field star contamination beyond the MS and at the red giants colour range.

Figures 5 and 6 are the colour-colour (CC) diagrams for stars with $(B-V)$ smaller and greater than 1.0 mag, respectively. In particular, the star distribution in Fig. 5 suggests the existence of variable absorption across the cluster field.

Membership in NGC 2323 has been determined by examining the positions of the individual stars in the CM and CC diagrams. Except for the red giants, cluster members were selected following the criteria described by Clariá & Lapasset (1986), namely by requiring the location of the star in both CM diagrams to correspond to the same evolutionary stage and that the location of the star in the CC diagram be close to the MS, the maximun departure accepted being 0.10 mag. Stars classified as probable members (m), possible members (pm) and non members (nm), are represented by filled circles, filled triangles and open circles in Figs. 3 to 6, respectively. Table 1 also includes the membership status assigned to each star.

Table 3. DDO data

Star	$C(45-48)$	$C(42-45)$	$C(41-42)$	n
12	1.402	1.140	0.220	2
	±0.002	±0.002	±0.016	
38	1.254	1.009	0.303	2
	0.007	0.004	0.017	
42	1.221	0.972	0.217	2
	0.011	0.005	0.022	
53	1.496	1.394	0.230	2
	0.006	0.013	0.016	
121	1.486	1.307	0.289	2
	0.008	0.020	0.002	

3.2. Foreground reddening

The reddening of NGC 2323 was determined from the brightest cluster members. According to Fig. 5, all member stars with $(U-B) < -0.49(B-V)+0.19$ are very likely earlier than the spectral type A2. Individual $E(B-V)$ and $E(U-B)$ colour excesses were derived for these stars from Eqs. (2) and (8) of García et al. (1988). The values of $E(B-V)$ and $E(U-B)$ for individual stars are listed in Table 4. The measured full width of the observed CC diagram from these stars is $\Delta E(B-V) = E_{\max}(B-V) - E_{\min}(B-V) = 0.16$ mag, which is larger than 0.11, the lower limit estimated by Burki (1975) for clusters with differential reddening. We conclude that the reddening across NGC 2323 is non-uniform. The mean values and standard deviations from 43 stars of Table 4 are: $< E(B-V) >= 0.252 \pm 0.054$,

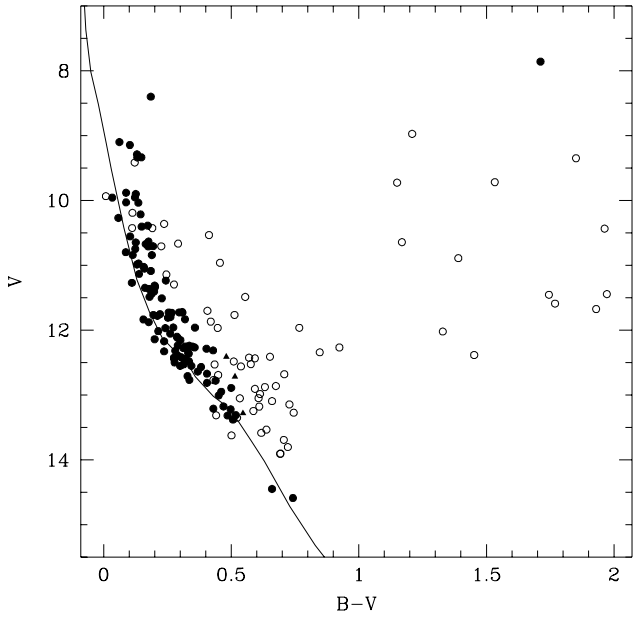

Fig. 3. The observed $V, (B - V)$ diagram for NGC 2323. Schmidt-Kaler's (1982) ZAMS has been adjusted to $E(B-V) = 0.25$ and $V - M_v = 10.62$

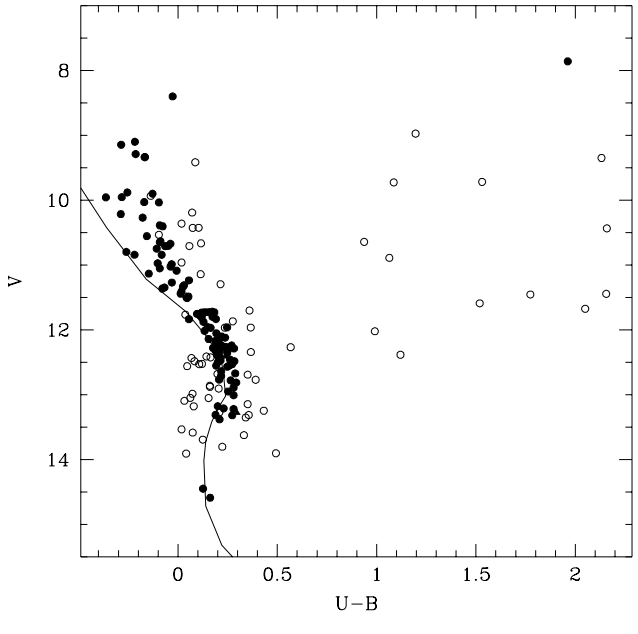

Fig. 4. The observed $V, (U - B)$ diagram for NGC 2323. Schmidt-Kaler's (1982) ZAMS has been adjusted to $E(U-B) = 0.17$ and $V - M_v = 10.62$

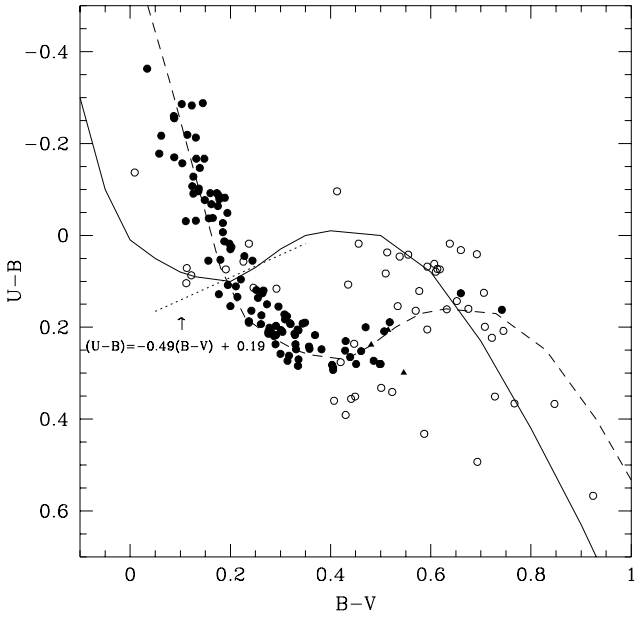

Fig. 5. Colour-colour diagram for stars with $(B - V) < 1.0$ mag in NGC 2323. Schmidt-Kaler's (1982) ZAMS has been plotted for $E(B-V) = 0.0$ (solid line) and $E(B-V) = 0.25$ (dashed line)

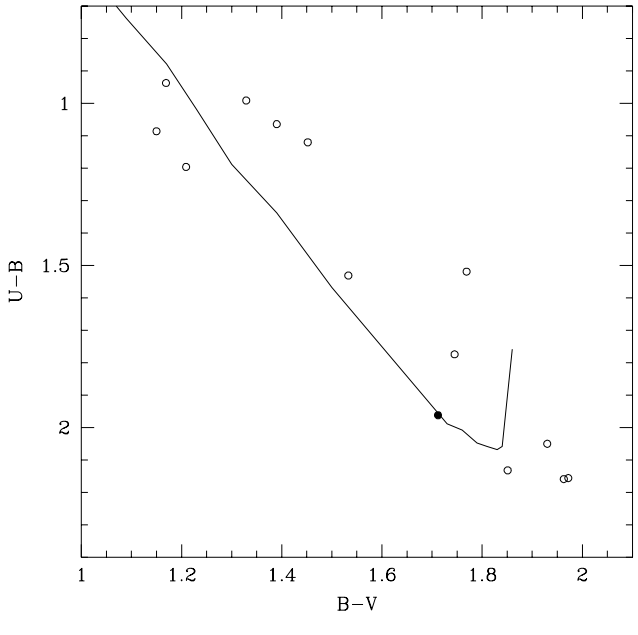

Fig. 6. Colour-colour diagram for stars with $(B - V) > 1.0$ mag. The solid line is the intrinsic relation of Schmidt-Kaler (1982) for luminosity class III stars

Table 4. Individual colour excesses for blue members

Star	$E(B-V)$	$E(U-B)$	Star	$E(B-V)$	$E(U-B)$
9	0.290	0.205	93	0.224	0.159
18	0.307	0.216	97	0.293	0.207
20	0.260	0.184	98	0.242	0.172
22	0.319	0.225	102	0.257	0.181
24	0.292	0.206	103	0.256	0.181
25	0.306	0.215	104	0.271	0.191
28	0.174	0.124	105	0.235	0.166
32	0.199	0.141	107	0.230	0.163
36	0.289	0.204	109	0.230	0.163
37	0.208	0.148	111	0.284	0.201
40	0.246	0.174	114	0.290	0.204
46	0.336	0.236	115	0.270	0.191
49	0.289	0.204	116	0.230	0.163
54	0.189	0.135	119	0.287	0.202
55	0.249	0.176	119'	0.274	0.193
69	0.280	0.197	123	0.252	0.178
73	0.303	0.214	137	0.223	0.158
74	0.292	0.206	138	0.265	0.188
81	0.279	0.197	151	0.260	0.184
82	0.256	0.181	*X*	0.263	0.186
88	0.279	0.197	*Z*	0.233	0.165
92	0.194	0.138			

$< E(U-B) >= 0.178 \pm 0.038$, which have been used in subsequent discussions. The resulting total visual absorption in front of the cluster is then 0.76 mag, assuming that $A_v/E(B-V) = 3.0$ (Clariá 1974).

The spatial correlation of reddening with position is shown in Fig. 7. Contrary to the north-south variation of reddening suggested by Schneider (1987) from Stromgrëm photometry of 10 stars, the interstellar material in front of NGC 2323 appears to be distributed following an irregular pattern. However, the mean $E(B-V)$ colour excess derived by Schneider agrees very well with our estimation. Other reddening determinations by different authors are also within the range $0.17 - 0.33$ mag. (e.g., Becker & Fenkart 1971; Mostafa et al. 1983), which are the lower and upper limits of the reddening distribution derived in this study.

3.3. Cluster distance

The ZAMS of Schmidt-Kaler (1982), appropiately reddened, can be fitted to the observed cluster sequence in the two CM diagrams by assuming an apparent distance modulus $V - M_v = 10.62$. The resulting true distance modulus is then $V_0 - M_v = 9.86$, which corresponds to a distance of 940 pc from the sun and 21 pc below the galactic plane.

The uncertainty in $E(B-V)$ is about 0.05 mag and the error in the fitting to the ZAMS is estimated to be 0.15 mag. Taking these uncertainties into account, we find that the cluster distance may be increased or decreased by about 10%.

There can be little doubt that some earlier distances of this cluster (e.g., Collinder 1931, 675 pc; Rieke 1935, 520 pc; Barkhatova 1950, 740 pc; Hoag et al. 1961, 1170 pc) were either over- or underestimated. However, we found a reasonable agreement with the estimations by Cuffey (1941) and Mostafa et al. (1983), who derived 910 pc and 995 pc, respectively.

3.4. Cluster diameter

To estimate the extent of NGC 2323, star counts in 2′.5 wide concentric circles around the cluster center adopted by Hoag et al. (1961) have been made. Numbers of stars per square arcmin as a function of the distance from the cluster center were counted to limiting magnitudes of $V = 10$, 11, 12, 13, 15 and ~ 17 (plate limit), the errors being estimated on the basis of Poisson statistics. The results for the counts down to $V = 10$ and for the V ranges: $10-11$, $11-12$, $12-13$ and $13-15$ are shown in Fig. 8. The following conclusions may be drawn from the star counts: (1) The star distribution for the different V intervals seems to be very similar, suggesting that the cluster has not suffered appreciable mass segregation effects. This is not the case, however, for the range $V = 13-15$ due to incompleteness of the data. (2) Cluster members are clearly concentrated in the central region within a radius of (10 ± 1) arcmin, which has been adopted for NGC 2323. (3) The adopted angular radius leads to a linear diameter of 5.46 pc, so that the minimum stellar density amounts to 1.28 stars pc^{-3}.

4. DDO analysis

The two CM diagrams of NGC 2323 reveal a relatively extensive and well-defined MS with the turn-off point in the late-B-star range and five yellow or red stars (see Table 3) which could be giant cluster members. The best method for separating red field stars from the physical members of the cluster is probably on the basis of proper motions and/or radial velocities, but these data are not available for NGC 2323. The selection process for red cluster members, however, can be performed by applying two photometric criteria (denoted A and B) described by Clariá & Lapasset (1983), which are based on combined BV and DDO data.

Before any interpretations may be made, DDO observed colours need correction for interstellar reddening. The $E(B-V)$ colour excesses were estimated for each star using the observed $(B-V)$, $C(45-48)$ and $C(42-45)$ colours and the iterative method described by Janes (1977). They are denoted $E(B-V)_{\rm GK}$ and listed in Col. (2) of Table 5, while Col. (3) gives the standard deviation $\sigma_{\rm E}$ computed using Eq. (2) of Clariá & Lapasset (1983). Star 53 was discarded in the following analysis because it falls outside Janes's (1977) calibration. The unreddened DDO colours were then obtained from $E(B-V)_{\rm GK}$ and the reddening ratios given by McClure (1976).

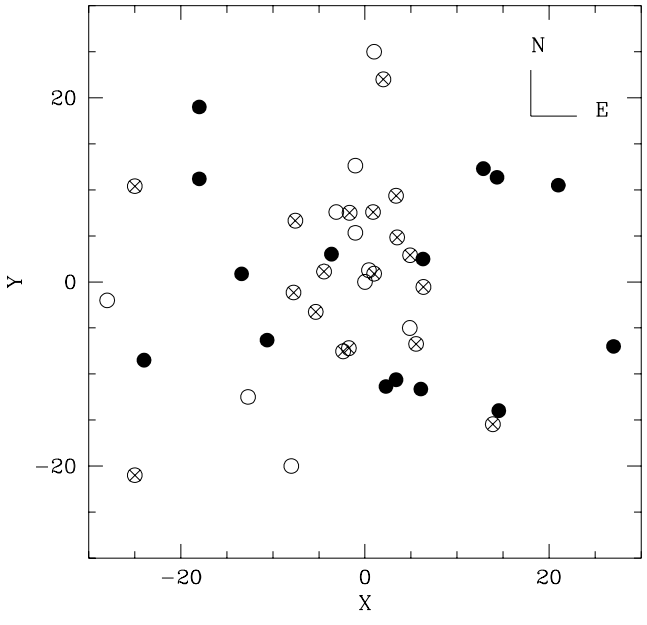

Fig. 7. $E(B-V)$ colour excesses of blue members plotted spatially. $E(B-V)$ ranges: $0.17-0.23$ (◯); $0.23-0.28$ (⊗); $0.28-0.33$ (full ◯). X, Y coordinates were taken from Hoag et al. (1961)

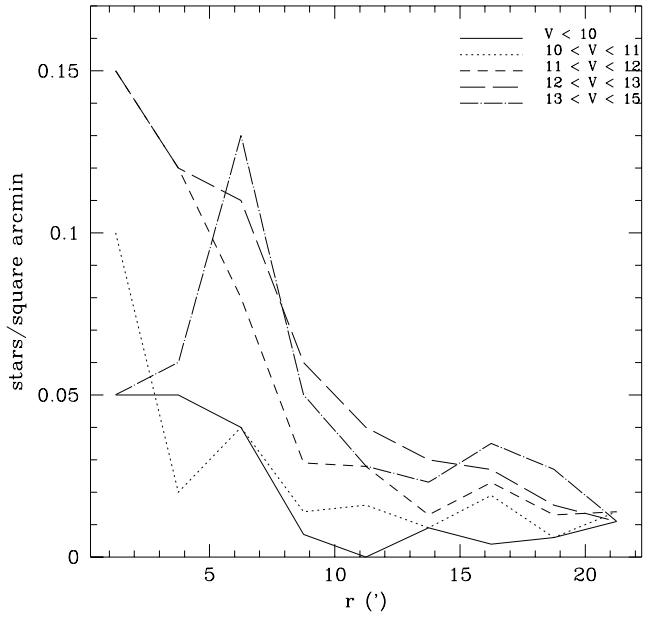

Fig. 8. Star counts for five limiting magnitudes in NGC 2323

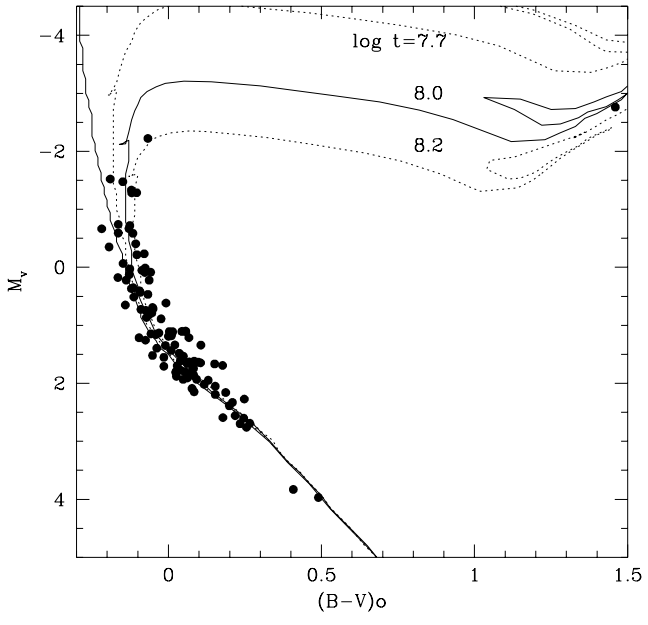

Fig. 9. M_v vs. $(B-V)_0$ diagram based on all stars believed to be cluster members. Isochrones corresponding to log $t = 7.7$, 8.0 and 8.2 (Bertelli et al. 1994) are plotted

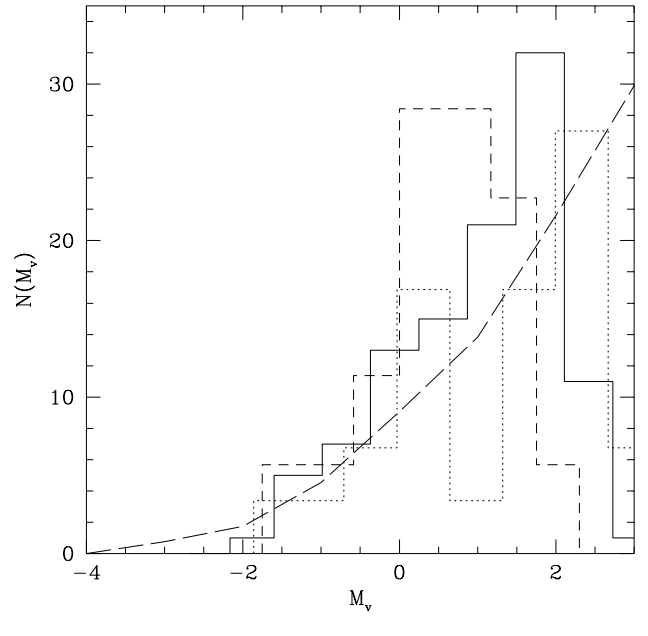

Fig. 10. Luminosity function of NGC 2323 (full histogram), compared to the normalized histograms of NGC 2335 (dashed histogram) and NGC 2343 (dotted histogram), and the Taff (1974) luminosity function (dashed line)

Table 5. Red giant membership results

Star	$E(B-V)_{GK}$	σ_E	MK(DDO)	Membership A	B	Adopted
12	0.244	0.027	K3/4 III	m	m	nm?
38	0.055	0.030	K2 III	nm	pm	nm
42	0.052	0.038	K2 III	nm	m	nm
121	0.237	0.037	K5 II-III	m	m	m

It is well known that the intrinsic $C_0(41-42)$ index of the DDO photometry measures the strength of the λ4216 band of cyanogen of G and K stars, so that the larger the index the greater the absorption by this band. We have computed the DDO cyanogen strength, ΔCN, for the stars of Table 5 by applying the procedure described by Piatti et al. (1993). By using Eq. (8) of Piatti et al. (1993) individual iron-to-hydrogen ratios were derived, which were in turn utilized to correct the intrinsic DDO colours for blanketing effects. The derived normal colours allowed us to assign MK spectral types to the stars using the calibration of Clariá et al. (1994). The derived MK spectral types are listed in Col. (4) of Table 5.

To discern whether or not a red star is a giant member, we applied the photometric criteria (A) and (B) proposed by Clariá & Lapasset (1983). To carry out this, we used the cluster reddening and distance modulus estimated in the present study. The results obtained from criterion (A) should be taken with caution because of the non-uniform reddening in the cluster field. The membership status derived from criteria (A) and (B) are presented in Cols. (5)-(6) of Table 5. As shown, according to the above mentioned criteria, stars 38 and 42 are likely foreground field giants, while stars 12 and 121 appear to be probable cluster members. In order to clarify the membership status of these two stars, we were greatly aided by the radial velocity observations of star 121 kindly provided by J.C. Mermilliod. Over a total of 11 CORAVEL measures of star 121, he obtained a mean radial velocity of 5.76 $\pm$ 0.10 km/s, in good agreement with the cluster radial velocity (9$\pm$3 km/s) published by Harris (1976). On the other hand, star 12 lies $\sim$ 1.0 mag below the isochrone of log $t = 8.0$ in the M_v vs. $(B-V)_0$ diagram (see Sect. 5), while the position of star 121 is clearly consistent with the cluster age. We then conclude that star 121 is the only giant member of NGC 2323.

5. Cluster age

The M_v, $(B-V)_0$ diagram for the probable members of NGC 2323 has been plotted in Fig. 9. Reddening and distance corrections have been applied to the observed CM diagram, using the adopted values for the $E(B-V)$ colour excess and apparent distance modulus. The cluster age was estimated by fitting theoretical isochrones computed by Bertelli et al. (1994), which include mass loss and moderate overshooting. Assuming a nearly solar metal content, we employed a set of isochrones corresponding to $Y = 0.28$ and $Z = 0.02$. Although star 121 is the only cluster member with derived metallicity ([Fe/H]DDO $= -0.37$), we believe that it may not be representative of the whole cluster.

In Fig. 9 we have drawn the ZAMS and the isochrones corresponding to log $t = 7.7$, 8.0, and 8.2 calculated by Bertelli et al. (1994). Both, evolutionary effects along the upper MS as well as the position of the only giant member (star 121) are satisfactorily reproduced by the isochrone corresponding to log $t = 8.0$. So that we have adopted an age for NGC 2323 of 100 Myr. This value is intermediate between those obtained by Barbaro et al. (1969) and Mostafa et al. (1983).

6. Luminosity function

The cluster luminosity function in terms of number of members in intervals of 0.5 mag width in absolute magnitude M_v is shown in Fig. 10 (full histogram). For comparison, the normalized luminosity functions of NGC 2335 (dashed histogram) and NGC 2343 (dotted histogram), as taken from Clariá (1973) and Clariá (1972), respectively, and that calculated by Taff (1974) (dashed line) from data of 62 well-studied open clusters, are also shown in Fig. 10.

Three important features should be noticed: (1) the number of stars per bin in NGC 2323 reaches its maximum and begins to decrease near $M_v = 2.0$. The maximum lies between the peaks of the histograms of NGC 2335 and NGC 2343. These two clusters aged 150 Myr and 110 Myr respectively (Clariá 1972, 1973) are located in the direction of CMa OB1 at nearly the same distance as NGC 2323. The turnover in the distribution for $M_v \geq 2.0$ is probably real since our cluster survey ceases to be complete for stars beyond a limiting magnitude of about $V = 13.5$, corresponding to $M_v = 2.9$. (2) Although the cluster histograms and the Taff luminosity function show in general a good agreement, the slope of the luminosity function in NGC 2323 appears to be somewhat steeper than in the Taff's function. (3) The three clusters lack stars brighter than $M_v = -2.0$.

7. NGC 2323 and the CMa OB1 association

NGC 2323 lies near the edge of CMa OB1 at 940 pc from the sun, i.e., scarcely nearer than the association, which is located at 1150 pc (Clariá 1974). However, the age derived for NGC 2323 (100 Myr) is much greater than that derived by Clariá (1974) for CMa OB1 (3 Myr). Therefore, it seems very improbable that NGC 2323 and CMa OB1 originated from the same protostellar material. The actual location of NGC 2323 could be explained taking into

Table 6. Summary of the results obtained for NGC 2323

Position		
$\alpha = 7^{\rm h}\ 00^{\rm m}8$	$\delta = -8^{\rm o}\ 16'$ (1950.0)	
$l = 221^{\rm o}\ 42'$	$b = -1^{\rm o}\ 18'$ (1950.0)	
Distance		
$V - M_v$	: apparent distance modulus	= 10.62
$E(B-V)$	: selective absorption	= 0.25 ± 0.05
A_v	: visual absorption (variable)	= 0.76
$V_0 - M_v$	: true distance modulus	= 9.86
d	: distance from the Sun	= 940 pc
z	: distance from the galactic plane	= −21 pc
Age		
log t	: log age	8.0
t	: age	100±20 My
Dimension		
D	: angular diameter	= 20'
δ	: linear diameter	= 5.46 pc
Luminosity function		
Maximum at $M_v \sim 2.0$		
Integrated parameters		
M_v	: visual absolute mag.	= -3.93
$(B-V)_0$	: intrinsic $(B-V)$ colour	= 0.16
$(U-B)_0$	: intrinsic $(U-B)$ colour	= −0.10
V_0	: visual magnitude	= 5.94
$M/M_\odot$	: total mass	> 285
π	: stellar density	= 1.3 star pc−3
ρ	: mean space density	≥ 3.3 $M_\odot$pc^{-3}

account the motion of the cluster along the galactic disk. In fact, it is possible to estimate the full period P for the expected oscillation of NGC 2323 around the galactic plane, using the expression: $P = 2\pi[K_z/z]^{-1/2}$, where K_z is the acceleration in the gravitational field perpendicular to the galactic plane, and z is the distance from the galactic plane (see, e.g., Trumpler & Weaver, 1953, paragraph 6.37). Adopting the acceleration K_z at $z = -21$ pc from the computed values for the solar neighbourhood (Bahcall 1984), then $P \approx 50$ Myr. Consequently, NGC 2323 could have been formed many years before the association in a region probably different from the one it occupies now, having crossed the galactic plane four times during its lifetime. Since its formation till the present NGC 2323 could have shifted to the region of the CMA OB1 association.

Table 6 summarizes the main results derived in this study.

Acknowledgements. We wish to thank J.C. Mermilliod for very generously providing unpublished radial velocity information. We are also happy to thank the Director, staff and technicians of Cerro Tololo Inter-American Observatory and Las Campanas Observatory for the allocation of observing time and for their kind assistance and hospitality. We gratefully acknowledge financial support from the Argentinian institutions CONICET, CONICOR and Fundación Antorchas.

References

Bahcall J.N., 1984, ApJ 276, 169
Barbaro G., Dallaporta N., Fabris G., 1969, Ap&SS 3, 123
Barkhatova K.A., 1950, AZh 27, 182
Becker W., Fenkart R.P., 1971, A&AS 4, 241
Bertelli G., Bressan A., Chiosi C., Fagotto F., Nasi E., 1994, A&AS 106, 275
Burki G., 1975, A&A 43, 37
Caillault J.P., 1994, ASP Conf. Proc. 313, "The soft X-ray cosmos. ROSAT Science Symposium", p. 7
Clariá J.J., 1972, AJ 77, 868
Clariá J.J., 1973, A&AS 9, 251
Clariá J.J., 1974, A&A 37, 229
Clariá J.J., Lapasset E., 1983, JA&A 4, 177
Clariá J.J., Lapasset E., 1986, AJ 91, 326
Clariá J.J., Lapasset E., Bosio M.A., 1991, MNRAS 249, 193
Clariá J.J., Piatti A.E., Lapasset E., 1994, PASP 106, 436
Collinder P., 1931, Ann. Lund Obs. 2
Cousins A.W.J., 1973, Mem. Royal Astron. Soc. 77, 223
Cousins A.W.J., 1974, MNASSA 33, 149
Cuffey J., 1941, ApJ 94, 55
García B., Clariá J.J., Levato H., 1988, Ap&SS 143, 317
Graham J.D., 1982, PASP 94, 244
Harris G.L.H., 1976, ApJS 30, 451
Henning T., Martin K., Launhardt R., Reimann H.G., 1995, Cologne-Zermatt Symposium, "The physics and chemistry of interstellar molecular clouds", p. 326
Hoag A.A., Johnson H.L., Iriarte B., Mitchell R.I., Hallam K.L., Sharpless S., 1961, Publ. US Naval Obs., Vol. XVII, part VII
Janes K.A., 1977, PASP 89, 576
Landolt, A.U., 1973, AJ 78, 959
McClure R.D., 1976, AJ 81, 182
McClure R.D., 1979, in "Problems of Calibration of Multicolour Photometric Systems", Philip A.G.D. (ed.). Dudley Observatory, p. 83
Massey P., Johnson K.E., DeGioia-Eaeswood K., 1995, ApJ 454, 151
Mostafa A.A., Hassan S.M., Aiad A., Ahmed T., 1983, Astron. Soc. Egypt 5, 23
Murray S.D., Lin D.N., 1996, ApJ 467, 728
Piatti A.E., Clariá J.J., Minniti D., 1993, JA&A 14, 145
Rieke C.A., 1935, Harvard College Observatory Circular 397
Schmidt-Kaler Th., 1982, in Landolt-Börnstein, Numerical Data and Functional Relationships in Science and Technology, New Series, group VI, Vol. 2b, Schaifers K. & Voigt H.H. (eds.). Berlin, Springer Verlag
Schneider H., 1987, A&AS 71, 531
Shaoguang L., 1995, Chin. Astron. Astrophys. 19, 316
Taff L.G., 1974, AJ 79, 1280
Trumpler R.J., Weaver H.F., 1953, Statistical Astronomy. Univ. Calif. Press., Berkeley